

The ISWI ATPase Smarca5 (Snf2h) Is Required for Proliferation and Differentiation of Hematopoietic Stem and Progenitor Cells

JURAJ KOKAVEC ^{a,b} TOMAS ZIKMUND,^a FILIPP SAVVULIDI,^a VOJTECH KULVAIT,^a WINFRIED EDELMANN,^b ARTHUR I. SKOULTCHI,^b TOMAS STOPKA^a

Key Words. Erythroid differentiation • Fetal liver erythropoiesis • Smarca5 • Imitation switch • Hematopoietic stem and progenitor cells • Cell cycle progression • p53 pathway • Hypoxia

^aBIOCEV, First Faculty of Medicine, Charles University, Czech Republic; ^bDepartment of Cell Biology, Albert Einstein College of Medicine, Bronx, New York, USA

Correspondence: Tomas Stopka, M.D., Ph.D., BIOCEV, First Faculty of Medicine, Charles University, Prumyslova 595, Vestec 25250, Czech Republic. Telephone: 42-032-587-3001; Fax: +420-32587-3001; e-mail: tomas.stopka@lf1.cuni.cz; or Arthur I. Skoultschi, Ph.D., Department of Cell Biology, Albert Einstein College of Medicine, 1300 Morris Park Ave., Bronx, New York 10461, USA. Telephone: 1-718-430-2169; Fax: 1-718-430-8574; e-mail: arthur.skoultschi@einstein.yu.edu

Received May 15, 2016; accepted for publication January 9, 2017; first published online in STEM CELLS EXPRESS March 9, 2017.

© AlphaMed Press
1066-5099/2017/\$30.00/0

<http://dx.doi.org/10.1002/stem.2604>

ABSTRACT

The imitation switch nuclear ATPase Smarca5 (Snf2h) is one of the most conserved chromatin remodeling factors. It exists in a variety of oligosubunit complexes that move DNA with respect to the histone octamer to generate regularly spaced nucleosomal arrays. Smarca5 interacts with different accessory proteins and represents a molecular motor for DNA replication, repair, and transcription. We deleted *Smarca5* at the onset of definitive hematopoiesis (*Vav1-iCre*) and observed that animals die during late fetal development due to anemia. Hematopoietic stem and progenitor cells accumulated but their maturation toward erythroid and myeloid lineages was inhibited. Proerythroblasts were dysplastic while basophilic erythroblasts were blocked in G2/M and depleted. Smarca5 deficiency led to increased p53 levels, its activation at two residues, one associated with DNA damage (S15^{Phos}) second with CBP/p300 (K376^{Ac}), and finally activation of the p53 targets. We also deleted *Smarca5* in committed erythroid cells (*Epor-iCre*) and observed that animals were anemic postnatally. Furthermore, 4-hydroxytamoxifen-mediated deletion of *Smarca5* in the *ex vivo* cultures confirmed its requirement for erythroid cell proliferation. Thus, Smarca5 plays indispensable roles during early hematopoiesis and erythropoiesis. STEM CELLS 2017;35:1614–1623

SIGNIFICANCE STATEMENT

Imitation switch chromatin remodeling ATPase Smarca5 is a highly conserved chromatin-remodeling factor that is expressed in hematopoietic tissues especially stem and progenitor cells. There exist several oligosubunit complexes containing *Smarca5* as a catalytic subunit that were previously shown to actively regulate nucleosomal structure and position during DNA replication, repair, and transcription. Genetic inactivation of *Smarca5* specifically in murine definitive hematopoietic cells leads to the developmental blockade marked by unique proliferative defects such as tetraploidy and erythroid dysplasia. The *Smarca5* gene is not mutated in cancer; however, its expression is enhanced in acute myeloid leukemia and aggressive solid tumors. These features may be utilized for development of future therapies to target the growth and spread of human malignancies.

INTRODUCTION

Nuclear DNA is carefully packaged into chromatin, a compact nucleoprotein complex that regulates many genomic activities. Imitation switch (ISWI) proteins are Sucrose non-fermenting 2 (SNF2)-like ATPases that facilitate chromatin assembly and remodeling through their DEAD/H helicase domains located close to their N-termini. Their C-termini contain SANT and SLIDE domains that recruit a variety of bromodomain-containing factors that recognize epigenetically modified histones. ISWI

proteins are integral units of several oligosubunit complexes that establish regularly spaced nucleosomes during DNA replication, cooperate with lesion-sensor proteins in DNA repair, and facilitate or inhibit transcriptional outcomes mediated by all three types of RNA polymerases (reviewed by Erdel and Rippe [1]).

The relatively large spectrum of Smarca5 activities is enabled by structural differences in the noncatalytic subunits that provide distinct contributions to sense the state of the DNA adjacent to nucleosomes [2]. Vertebrate ISWIs

are represented by two homologues: *Smarca5* (Snf2h) and *Smarca1* (Snf2l). While *Smarca5* is expressed in stem and progenitor cells as well as in undifferentiated tumor cells, *Smarca1* is expressed only at later stages suggesting that *Smarca5* may be required at early stages of development when cell fate is being decided [3]. The blood system and especially erythroid cells are the most highly *Smarca5*-expressing tissues.

Hematopoietic stem cells (HSCs) possess great potential to self-renew throughout life and to give rise to several types of multipotent progenitors (MPPs), which then differentiate along myeloid or lymphoid pathways to produce sufficient amounts of the various mature specialized blood cells. Lineage-specific transcription factors cooperate with additional factors and are often involved in epigenetic modification that is necessary to promote differentiation of self-renewing stem cells. Transcriptional regulation of early hematopoiesis has been reported to involve the SWI/SNF2-like proteins. For example, a hypomorphic mutation of the murine *Brg1* ATPase results in anemia, embryonic day (E) 14.5 lethality and a blockade at the polychromatic erythroblast stage [4]. Our previous work suggested that *Smarca5* is also involved in the regulation of hematopoiesis. Inhibiting its levels in human CD34+ progenitors suppresses cytokine-induced erythropoiesis in vitro [5]. Conventional knockout of murine *Smarca5* is lethal very early in embryonic development—long before primitive hematopoiesis is established [5], thus preventing a determination of its role in hematopoiesis. In this article, we describe new conditional *Smarca5* knock-out mouse model and use it to determine how loss of *Smarca5* affects hematopoiesis. Our results show that loss of *Smarca5* disrupts definitive hematopoiesis in the fetal liver (FL), causing anemia due to defects in proliferation and differentiation of both HSCs and MPPs. *Smarca5* also is required for proliferation and survival of fully committed erythroid progenitors (EPs).

MATERIALS AND METHODS

Generation of *Smarca5* Knock-out Mice and Cells

The *Smarca5* targeting construct contained three 129Sv-derived murine genomic DNA fragments: (a) the 5' homology arm (1.5 kb *PmeI-HindIII* containing exon4), (b) the targeted *HindIII-HindIII* region (~1 kb with exon5 surrounded by loxP sites (*flox5*; deletion of which would create a frame shift), and (c) the 3' homology arm (4.5 kb *HindIII-HindIII* containing exons 6–8) (Supporting Information Fig. S1A). The construct was electroporated into WW6 embryonic stem cells and 2 of 12 independent clones were injected into C57Bl/6 blastocysts as described recently [6]. Detection of the targeted allele was determined by polymerase chain reaction (PCR) amplification of a 3' loxP-containing fragment followed by cleavage at a unique (*Ascl*) restriction site (Supporting Information Fig. S1B). The floxed *Smarca5* allele can be detected by conventional PCR (Supporting Information Fig. S1C). Germline deletion using *Zp3-Cre* transgene [7] produced *Smarca5*^{+/Δ5} heterozygous mice that displayed reduced *Smarca5* protein levels. While the *Smarca5*^{flox5/flox5} mice were fertile and viable, the progeny of *Zp3-Cre*-dependent germline inactivation recapitulated the early perimplantation lethality as described previously in *Smarca5*^{Δ5-9/Δ5-9} mice [5]. Thus, deletion of exon5

results in a null allele (Supporting Information Fig. S1E). Methods for Supporting Information Figure S1C are provided in the Supporting Information. The Institutional Ethical Board and law on GMO approved mice handling. Mouse E12.5 FL-derived *Smarca5*^{flox5/Δ5-9} *Cre-Esr1* EPs (FL-EPs) or *Smarca5*^{flox5/flox5} were cultivated [8] and treated by 1 μM 4-hydroxytamoxifen (4-OHT) (*Tg(CAG-cre/Esr1*^{tax}^{5Amc}) [9] or diluent (ethanol) alone.

Cell Cycle, Clonogenic, and Apoptosis Assays

In vivo 5-Bromo-2'-deoxyuridine (BrdU) staining for 1 hour was analyzed by flow cytometry (see Supporting Information) on BD Canto II flow analyzer and analyzed by FlowJo software (TreeStar Inc., Ashland, OR, www.flowjo.com). Colony forming unit (CFU) assay used Methocult M3434 (StemCell Technologies, Vancouver, BC, Canada, www.stemcell.com). Approximately 4 × 10⁴ FL cells were plated. Apoptosis assay used immunofluorescence (IF) of cleaved Caspase-3 and Terminal deoxynucleotidyl transferase (TdT) dUTP Nick-End Labeling (TUNEL) assays (Supporting Information).

Gene Expression

Cell staining by H&E on histology sections and cytology smears (May–Grünwald–Giemsa) is described in the Supporting Information. Surface marker detection (FACS Canto II, BD Biosciences, San Jose, CA, www.bdbiosciences.com) used conjugated antibodies and published protocols [10, 11]. The microarray analysis used Affymetrix GeneChip Mouse Genome 430 2.0 Array (Affymetrix, Santa Clara, CA, www.affymetrix.com). Probes were accepted differentially expressed on False Discovery Rate (FDR) adjusted *p* < .01 (for more details see Supporting Information). Link to the expression data may be found in Gene Expression Omnibus database, www.ncbi.nlm.nih.gov/geo. Protocols and the antibodies used for western blotting, IF, and flow cytometry are listed in the Supporting Information. Briefly, whole protein lysates from E13.5 or E14.5 FLs were prepared in Radioimmunoprecipitation assay (RIPA) buffer supplemented with proteinase and phosphatase inhibitors. Blocking and staining was performed in Tris-buffered saline/0.1% Tween-20 with 5% milk or 3% bovine serum albumin with antibody dilutions following manufacturer's recommendations. Immunoblots were visualized by ChemiDo MP System (Bio-Rad, Hercules, CA, www.bio-rad.com).

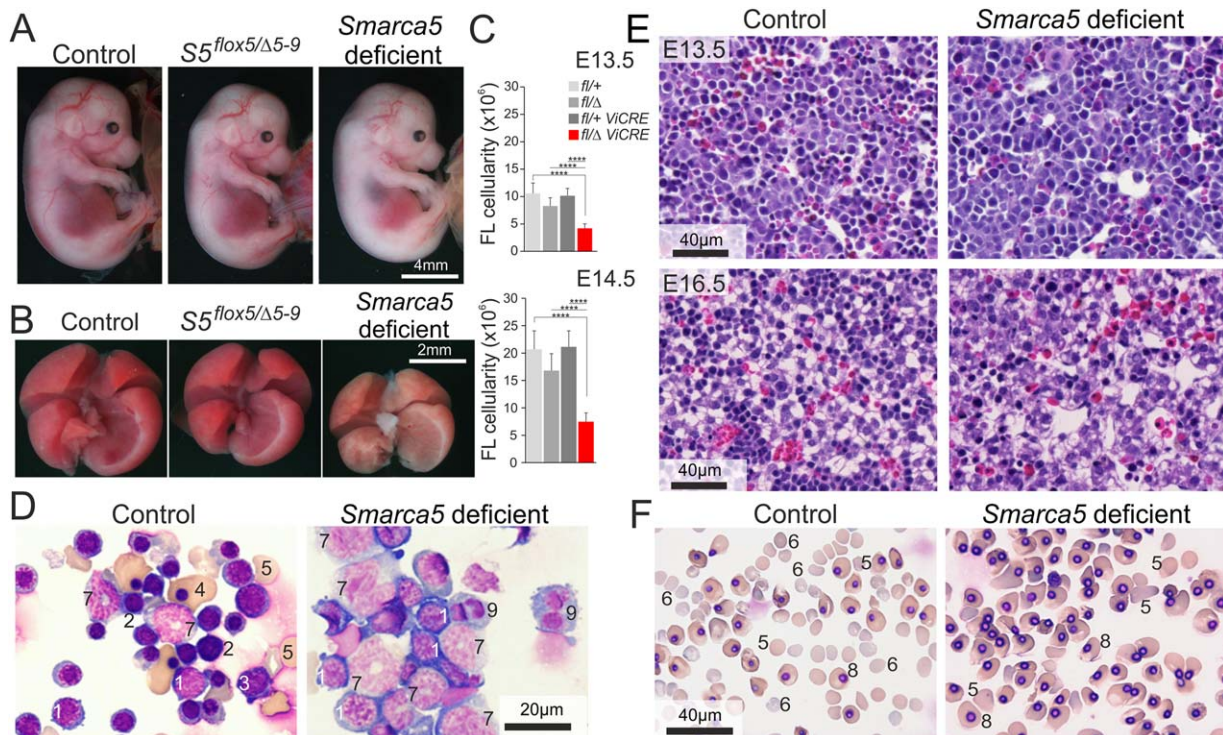
RESULTS

Smarca5 Is Required for Definitive Hematopoiesis

We reported previously that *Smarca5* null mouse embryos die shortly after implantation [5]. To investigate the role of *Smarca5* in later development, we produced a conditional knock-out allele by inserting LoxP1 sites in introns 4 and 5 (Supporting Information Fig. S1A). The *Cre*-recombinase-mediated removal of exon5 in the *Smarca5*^{flox5} allele is predicted to result in a null allele due to removal of a portion of the catalytic ATPase domain, also creating a frameshift and premature stop codon. *Smarca5*^{flox5/flox5} mice were viable, fertile, and developed normally. To study the role of *Smarca5* at the onset of definitive hematopoiesis, we used a transgene that expresses iCre recombinase driven by the *Vav1*-promoter. *Vav1* is a target of the stem cell factor receptor (c-Kit) signaling [12] and is activated in

Table 1. Distribution of genotypes in utero at embryonic (E12.5–E18.5) and postnatal stages in the progeny of *Smarca5*^{+/Δ5-9}*Vav1-iCre* and *Smarca5*^{fllox5/fllox5} mice

Developmental stage	<i>Smarca5</i> ^{fllox5/+}		<i>Smarca5</i> ^{fllox5/Δ5-9}		Total
	(%)	<i>Vav1-iCre</i> (%)	(%)	<i>Vav1-iCre</i> (%)	
E12.5	11 (28.9)	10 (26.3)	11 (28.9)	6 (15.8)	38
E13.5	92 (27.4)	71 (21.1)	82 (24.4)	91 (27.1)	336
E14.5	48 (23.5)	55 (27.0)	50 (24.5)	51 (25.0)	204
E15.5	15 (27.8)	9 (16.7)	15 (27.8)	15 (27.8)	54
E16.5	10 (23.8)	12 (28.6)	9 (21.4)	11 (26.2)	42
E17.5	4 (16.0)	8 (32.0)	7 (28.0)	6 (24.0)	25
E18.5	9 (21.4)	10 (23.8)	10 (23.8)	12 (28.6) ^a	41
E12.5–E18.5	189 (25.5)	175 (23.6)	184 (24.9)	192 (25.9)	740
Postnatal	32 (37.2)	30 (34.9)	24 (27.9)	0 (0.0)	86

^aNonviable embryos.**Figure 1.** *Smarca5* deletion (*Vav1-iCre*) results in anemia. (A): Phenotypic appearance of control *Smarca5*^{fllox5/+} (left), heterozygous *Smarca5*^{fllox5/Δ5-9} (middle), and *Smarca5* deficient *Smarca5*^{fllox5/Δ5-9} *Vav1-iCre* (right) sibling embryos at embryonic day (E)15.5. (B): E15.5 fetal livers (FLs) of the same genotypes. (C): FL cellularity (E13.5 upper, E14.5 lower) of control *Smarca5*^{fllox5/+}, *Smarca5*^{fllox5/Δ5-9}, and mutant *Smarca5*^{fllox5/Δ5-9} *Vav1-iCre* embryos. (D): Cytology (May-Grünwald-Giemsa) of E14.5 FL and (E) histology (H&E) of E13.5 (top) and E16.5 FLs (bottom). (F): Cytology (May-Grünwald-Giemsa) of E14.5 peripheral blood. Cell subtypes: (1) proerythroblast, (2) basophilic normoblast, (3) polychromatic n., (4) orthochromatic n., (5) reticulocyte, (6) erythrocyte, (7) myeloid precursor, (8) embryonic erythrocyte, and (9) atypical double-nucleated cell. Similar results were obtained in at least six repeat experiments. Two-tailed Student's *t* test (****, *p* < .00001). Abbreviation: E13.5/14.5, embryonic day 13.5/14.5.

definitive HSCs starting at E10.5 [13]. *Vav1-iCre* transgenic mice were bred with *Smarca5*^{+/Δ5-9} mice described previously [5] to produce the *Smarca5*^{+/Δ5-9}*Vav1-iCre* strain. This strain was then mated with *Smarca5*^{fllox5/fllox5} mice. We observed that mice with the genotype *Smarca5*^{fllox5/Δ5-9} *Vav1-iCre* are not born; other genotypes (*Smarca5*^{fllox5/+}, *Smarca5*^{fllox5/+} *Vav1-iCre*, and *Smarca5*^{fllox5/Δ5-9}) were produced in the expected numbers (Table 1).

Analysis of embryos between days E11.5–18.5 indicated that all *Smarca5*^{fllox5/Δ5-9} *Vav1-iCre* embryos are pale—the effect is apparent at E14.5 (Supporting Information Fig. S1F) and even more apparent at E15.5 (Fig. 1A). Mutant embryos display significantly smaller FLs (Fig. 1B; Supporting Information Fig. S1G)

and decreased FL cellularity (Fig. 1C). In contrast, FL development in *Smarca5*^{fllox5/Δ5-9} mice is normal (Fig. 1B, 1C, middle panels), suggesting that the single *Smarca5*^{fllox5} allele is not hypomorphic. By E18.5, all mutant embryos die in utero with subcutaneous swelling indicative of hemodynamic failure (Supporting Information Fig. S1H; Table 1). Cytological examination of *Smarca5*^{fllox5/Δ5-9} *Vav1-iCre* FLs between E12.5 and E14.5 revealed a lack of maturing erythroid cells, whereas control FLs contained all stages of maturing erythroid cells (Supporting Information Fig. S1D, S1I). The histologic examination of E13.5 and E16.5 mutant FLs confirmed that the *Smarca5*^{fllox5/Δ5-9} *Vav1-iCre* FLs display disrupted structure of acinus and depletion of maturing erythroid cells in favor of immature HSCs (Fig. 1E;

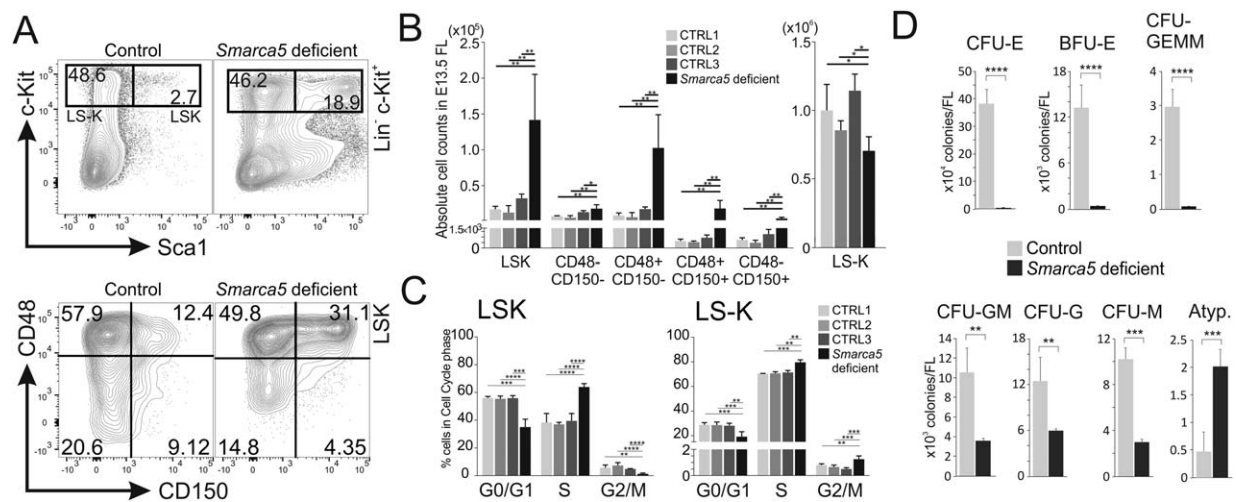


Figure 2. *Smarca5* deletion (*Vav1-iCre*) disturbs early hematopoiesis. **(A)** Flow cytometry analysis of control (*Smarca5*^{flx5/+} *Rosa26*^{eYFP/+} *Vav1-iCre*) and mutant *Smarca5*^{flx5/Δ5-9} *Rosa26*^{eYFP/+} *Vav1-iCre* embryonic day 13.5 (E13.5) fetal liver (FL) with relative proportions of Sca1⁺ or Sca1⁻ cells within the c-kit⁺ lin⁻ cells. Gating of Lin- and c-Kit cells, which are subdivided into Lin- Sca1⁻ c-Kit⁺ (LS-K) and Lin- Sca1⁺ c-Kit⁺ (LSK) populations were enriched for hematopoietic progenitors. LSKs are further subdivided according to CD48 and CD150 expression. **(B)** Absolute numbers of LSK and LS-K cell populations in E13.5 FL determined as a number of CD48⁺ and/or CD150⁺ LSK events per total FL cells that were analyzed. Controls: (1) *Smarca5*^{flx5/+} *Rosa26*^{eYFP/+}; (2) *Smarca5*^{flx5/Δ5-9} *Rosa26*^{eYFP/+}; (3) *Smarca5*^{flx5/+} *Rosa26*^{eYFP/+} *Vav1-iCre*; and mutant *Smarca5*^{flx5/Δ5-9} *Rosa26*^{eYFP/+} *Vav1-iCre*. **(C)** Cell cycle progression in LSK and LS-K cell populations in E13.5 FL. **(D)** Colony forming assay of hematopoietic progenitors derived from E13.5 FL of *Smarca5*^{flx5/+} *Rosa26*^{eYFP/+} *Vav1-iCre* and mutant *Smarca5*^{flx5/Δ5-9} *Rosa26*^{eYFP/+} *Vav1-iCre* embryos scored by day 9 according to standard procedures. Similar results were obtained in at least six repeat experiments. Two-tailed Student's *t* test (*, *p* < .05; **, *p* < .001; ***, *p* < .0001; ****, *p* < .00001). Abbreviations: BFU, Burst-forming unit; CFU, colony forming unit; CTRL, control; LSK, Lin- Sca1⁺ c-Kit⁺; LS-K, Lin- Sca1⁻ c-Kit⁺.

Supporting Information Fig. S1J). *Smarca5*^{flx5/Δ5-9} *Vav1-iCre* FLs frequently displayed dysplastic changes such as atypical and often binucleate proerythroblasts (Fig. 1D; Supporting Information Fig. S1J). Erythroid hypogenesis in the mutant FLs was reflected in the peripheral blood (PB) smears at E14.5 (Fig. 1F) and E15.5 (Supporting Information Fig. S1K) which showed decreased numbers of definitive (non-nucleated) erythrocytes. Instead, the PB contained large numbers of nucleated erythrocytes, indicating a defect in the embryonic-to-definitive erythropoiesis switch. HSCs at E15.5 stage control FLs expressed *Smarca5*, but this was not observed in the mutant FLs by immunostaining (Supporting Information Fig. S1L). These results indicate that *Smarca5* loss abrogates definitive hematopoiesis within FL, leading to anemia and E18.5 lethality.

***Smarca5* Deficiency Disturbs Proliferation and Differentiation of Hematopoietic LSK and LS-K Progenitors**

Because *Vav1-iCre* is active at the earliest stages of definitive hematopoiesis [13], we could investigate the consequences of *Smarca5* deficiency in very early HSCs. We assessed hematopoiesis of the E13.5 FL via flow cytometry using stem cell (Sca1, c-Kit) and SLAM (CD48, CD150) antigens in lineage-negative FL cells as reported previously (Supporting Information Fig. S2A) [11, 14]. Lin- Sca1⁺ c-Kit⁺ (LSK) cells are defined as Sca-1 and c-Kit-expressing cells which are depleted of lineage-positive marker expression, while the Lin- Sca1⁻ c-Kit⁺ (LS-K) cells are those that lack expression of Sca-1 but are positive for c-Kit and negative for lineage markers. In absolute numbers, the mutants were greatly enriched in LSK cells but not in LS-K (Supporting Information Fig. S2A; Fig. 2B). Further analysis using SLAM antigens revealed an increase in the absolute number of MPP cells including the

earliest MPP-1 (LSK⁺CD48⁻CD150⁺), myeloid-biased MPP-2 (LSK⁺CD48⁺CD150⁺), MPP-3 (CD48⁺CD150⁻) with myelolymphoid potential, as well as the Ery/Mk-biased LSKs (CD150⁻CD48⁺) (Fig. 2B). The Ery/Mk-biased LSKs represent the short repopulating stress-responsive MPPs [15]. In contrast to absolute numbers of the MPP cells, the relative numbers of MPP cells were not disturbed except for an approximate 2.5-fold increase in the myeloid-biased MPP-2 fraction (Fig. 2A, bottom). To gain insight into the cell cycling of the accumulated MPP populations, we used *in vivo* BrdU labeling in E13.5 embryos. We found that the percentage of mutant E13.5 LSK cells in S-phase was increased relative to controls, whereas the percentage of these cells in G0/G1 and G2/M phases was decreased (Fig. 2C, left). This phenomenon was observable for all analyzed MPP subpopulations (Supporting Information Fig. S2C). This suggests that *Smarca5* deletion induced proliferation of all types of the mutant LSK cells. In contrast, the mutant committed progenitors within the LS-K compartment (together with less pronounced increase in S-phase) exhibited significantly increased proportion of blocked cells in G2/M phase suggesting that upon differentiation more *Smarca5*-negative cells became inhibited in proliferation.

To test the proliferative potential of committed FL-derived progenitors, we used a CFU assay in methylcellulose semisolid media. While FL-derived progenitors from control E13.5 embryos formed colonies of erythroid (BFU-E, CFU-E), myeloid (CFU-GM, CFU-GG, CFU-M), or mixed (CFU-GEMM) potential, formation of these colonies by the *Smarca5*^{flx5/Δ5-9} *Vav1-iCre* FL progenitors was severely reduced (Fig. 2D; Supporting Information Fig. S2D). The effect of *Smarca5* deletion was more severe within the erythroid lineage, whereas formation of myeloid colonies was only partially affected. However, the surviving myeloid colonies displayed grossly atypical

morphology. The atypical morphology in the mutants included dysplastic features such as cell size and cell shape differences and unevenness within one colony as well as atypical appearance and cellularity of individual colonies. To determine whether the atypical mutant myeloid colonies underwent *Cre*-mediated deletion, we used a mouse strain containing a *Rosa26-STOP-eYFP* reporter allele. Upon deletion of a transcription terminator signal by *iCre-recombinase*, this strain produces eYFP fluorescence detectable by flow cytometry [16]. Indeed, as indicated by positive eYFP fluorescence, these surviving colonies expressed *iCre*, suggesting that the atypical morphology is a result of *Smarca5* gene deletion (Supporting Information Fig. S2D). In summary, these results indicate that the number of HSCs in *Smarca5*-deficient embryos is increased due to excessive cycling but their progeny, the MPPs, are blocked in their maturation.

Smarca5 Deficiency Leads to Induction of the p53 Target mRNAs in Hematopoietic Progenitors

We sought insights into the maturation defect in the mutant progenitor population by investigating their gene expression profile. We compared the levels of 39,000 transcripts in mutant (*Smarca5*^{Δ5/Δ5-9} *Vav1-iCre*) and control FL-derived magnetically sorted Kit⁺ progenitors from E15.5 embryos by hybridization to Affymetrix GeneChip Mouse Genome 430 2.0 Array with 45,101 probes. Probes were accepted differentially expressed on FDR adjusted $p < .01$. Using this approach, we found 2,252 downregulated and 1,403 upregulated probes. Many of the most significant, differentially expressed gene sets among GO Biological Process categories link to response to stress, DNA damage, repair, and apoptosis, and also to hypoxia (Fig. 3A, 3B; Supporting Information Fig. S3A, S3D).

According to the DAVID annotation tool, many of the genes in the KEGG p53-signaling pathway are significantly, differentially expressed in *Smarca5*^{Δ5/Δ5-9} *Vav1-iCre* versus control progenitors (Fig. 3B). Changes in p53 pathway mRNAs are often associated with DNA damage and may result in apoptotic signaling-induced DNA fragmentation. To assess this, we used the TUNEL assay. The results showed that indeed mutant FLs exhibited a higher frequency of TUNEL-positive cells (Supporting Information Fig. S3B). To quantify the frequency of apoptotic cells in the mutants, we determined the level of cleaved Caspase-3 in the FLs at E16.5 stage. The data show that the mutant FLs activated Caspase-3, while the control FLs showed very low frequency of Caspase-3-positive cells (Fig. 3C). These data are consistent with upregulation of Caspase-3 mRNA level in the mutant FL progenitor cells (see Fig. 3B).

To address whether by deleting *Smarca5* at early progenitor stages, the DNA damage response (DDR) pathways became activated, we tested DDR-dependent events including the levels of p53 and its S15^{Phos} modification which was previously associated with DDR activation [17]. We also assessed acetylation of Lysine (K) 376 of p53 (homologous to human K382) which is mediated by p300/CBP acetylases [18]. First, we observed that the irradiated mutants expressed slightly higher level of p53 compared with controls and the level of its inhibitor Mdm2 was reciprocally decreased (Fig. 3D). Target of p53, *Ccnd2*, was also increased in the mutants. Second, we also detected an increase in two p53 modifications in the mutants: S15^{Phos} and K376^{Ac} (Fig. 3D). Additional control on the Western blots included expression of *Smarca5* that again confirmed that no gene product is made from the mutant

allele. Next, to further study whether the *Smarca5* mutants display DNA damage, we determined γ H2AX foci and p53BP1 expression using fluorescent microscopy. However, neither of these two marks were positive in the *Smarca5* mutants or control FLs unlike in the positive control (irradiated wild-type thymus, Supporting Information Fig. S3E) supporting the possibility of more complex activation of p53. We conclude that *Smarca5* deficiency activated p53 at two residues, one associated with DNA damage (S15^{Phos}) and another with CBP/p300 (K376^{Ac}).

Smarca5 Deficiency Leads to Perturbations in Cell Cycle Progression and Inhibition of Erythroid Differentiation

The foregoing results indicate that *Smarca5*-deficient HSCs are able to differentiate to the MPP stage but that these progenitors are limited in their ability to mature into committed HSCs. To further investigate the causes of the block to terminal erythroid differentiation, we analyzed various stages of erythroid cell maturation within the developing FL. CD71 and Ter119 cell surface markers and flow cytometry [10] can be used to quantify cells of increasing maturation within the erythroid compartment, from the least mature cells (S0) to the terminally differentiated cells (S4 and S5) (Supporting Information Fig. S4A). Flow cytometry analyses showed that at E13.5, the *Smarca5*^{lox5/Δ5-9} *Vav1-iCre* FLs exhibit a higher proportion of S0 progenitors (26% vs. 6% in controls) and their immediate progeny (S1: 7% vs. 1%; S2: 9% vs. 6%) and a reduced proportion of the more mature S3 cells (35% vs. 69% in controls) (Fig. 4A; left panel). This shift toward immature stages is also seen in the absolute numbers of the S0 and S1 FL erythroid populations. (Fig. 4A; right panel). In contrast, there is a marked reduction in the absolute numbers of the more mature S3–S5 cells. Using the *Rosa26-STOP-eYFP* reporter allele, we show that *Vav1-iCre* is expressed in several FL erythroid cell populations (Supporting Information Fig. S4B; lower panel).

The observed shift toward immature stages in the mutant could be due to defects in cell proliferation, cell differentiation, or cell survival. To investigate cell proliferation, we used in vivo BrdU labeling and also scored the DNA content of the cells by flow cytometry after staining with 7-aminoactinomycin D (7-AAD). The E13.5 pregnant females were injected with BrdU and the FLs of the embryos were removed and analyzed for hematopoietic markers. We observed a marked decrease in the proportion of cells in S-phase in the mutant S3 population and a significant increase in cells in G2/M in the mutant S2–S5 populations. Particularly noteworthy was a marked increase in the polyploidy of G2/M cells in the mutant S3 population (Fig. 4B) not seen in controls (Supporting Information Fig. S4C). Thus, *Smarca5* deficiency leads to perturbations in cell cycling within the FL erythroid populations, including accumulation of cells with abnormal ploidy.

To assess the differentiation properties of the mutant cells, we used reverse transcriptase (RT)-PCR to analyze the mRNA levels of several key transcription factor genes involved in erythropoiesis. We used the *Rosa26-STOP-eYFP* allele to isolate eYFP-positive S0–S3 cells, which underwent *Vav1-iCre*-mediated deletion. We observed a strong reduction in *Gata2* mRNA in the mutant S0 cells, and significant reductions in *Gata1*, *Klf1*, and *Nfe2* mRNAs in the mutant S3 cells (Fig. 4C). We also assessed the expression of erythroid target genes,

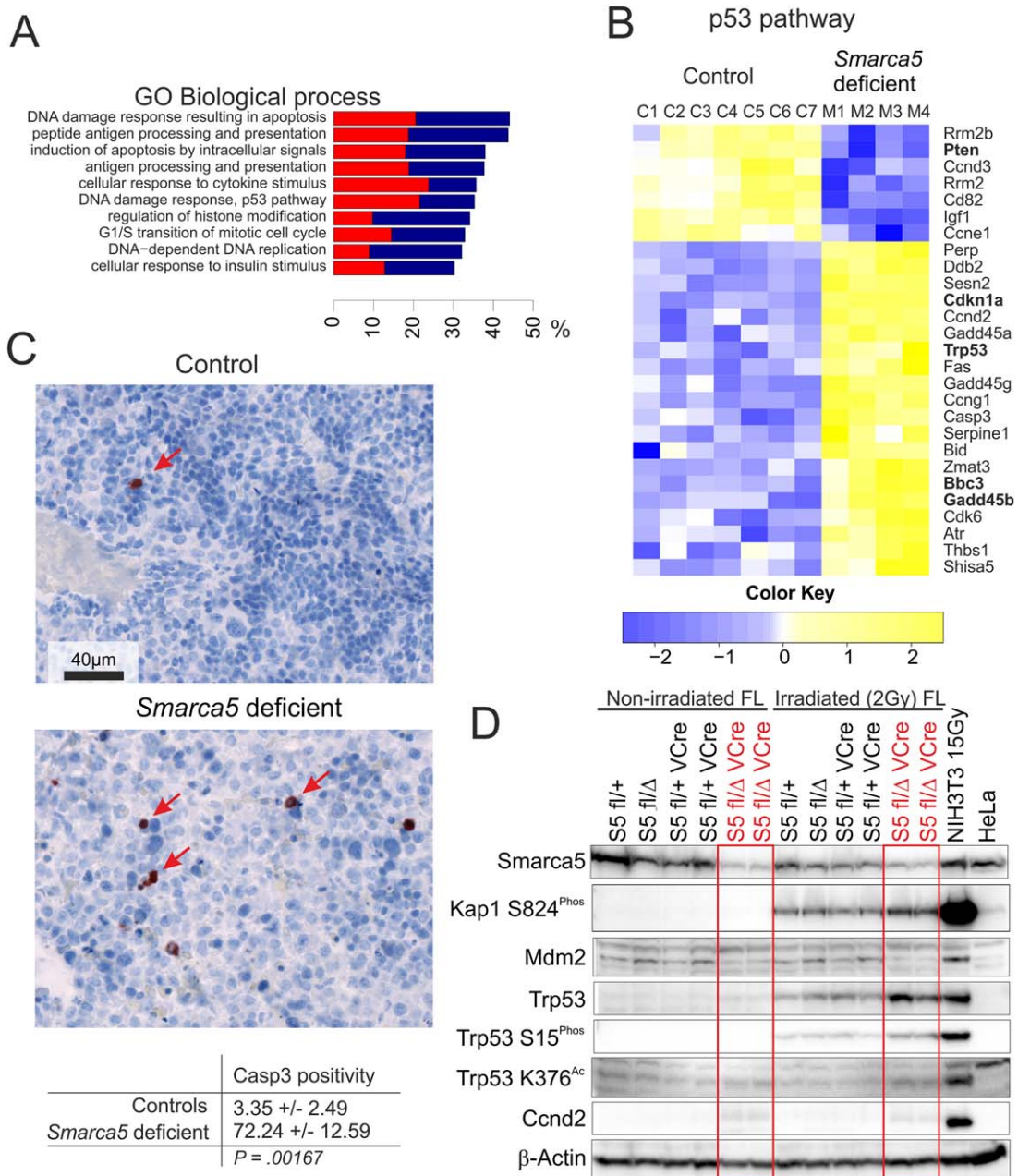


Figure 3. *Smarca5*-deleted progenitors express DNA damage mRNAs. **(A)**: The 10 most significantly enriched categories in GO Biological Process database with 20–500 member genes according to Fisher’s exact test and Z-test both with FDR corrected significance below $p = .05$. The x-axis represents a share of differentially regulated genes in a given category. Downregulated genes are represented as blue and upregulated as red. **(B)**: Heatmap of differentially regulated genes involved in the KEGG p53-signaling pathway. Upregulation (yellow), downregulation (blue), scale indicates the fold change. Mutants: *Smarca5*^{fl^{ox5}/Δ5-9} *Vav1-iCre* *c-kit*⁺ samples ($N = 4$); controls ($N = 7$). The genes in bold were also measured in Supporting Information Figure S4E. **(C)**: Immunofluorescence for cleaved Caspase-3 in the E16.5 fetal liver (FL) ($n = 7$). Caspase-3 positivity per 1 mm² is shown. Arrows indicate positive signals. **(D)**: Immunoblots of FL lysates of *Smarca5*^{fl^{ox5}/Δ5-9} *Vav1-iCre* (within red rectangles) and controls either irradiated (2Gy) or nonirradiated. Irradiated NIH3T3 (15Gy) or HeLa cells were used as controls. Similar results were obtained in at least two repeat experiments. Abbreviation: FL, fetal liver.

including *Epor*, *Alas2*, and globins. Indeed, expression of definitive globin (*Hba-a1* and *Hbb-b1*) mRNAs and the erythroid-specific *Alas2* and *Epor* genes was significantly reduced in the mutants. Interestingly, expression of embryonic globin (*Hba-x* and *Hbb-y*) mRNAs was increased, indicating a developmental delay of erythropoiesis in the mutant (Supporting Information Fig. S4D). In addition, no compensatory increase in *Smarca5* homolog *Smarca1* was observed (Supporting Information Fig. S4D). To determine the survival properties of the mutant cells,

we used AnnexinV and propidium iodide staining by flow cytometry and found that FL cells lacking *Smarca5* contain an increased proportion of apoptotic (5% in controls vs. 7% in mutants) and necrotic (3% vs. 9%) cells (Fig. 4D).

To assess whether the DDR pathway is involved in the shift to a more immature erythroid population in the mutant, we measured the levels of several of the DDR mRNAs identified in the microarray analysis of *Kit*⁺ cells (Fig. 3B, in bold). We used quantitative RT-PCR to analyze mRNA levels in the

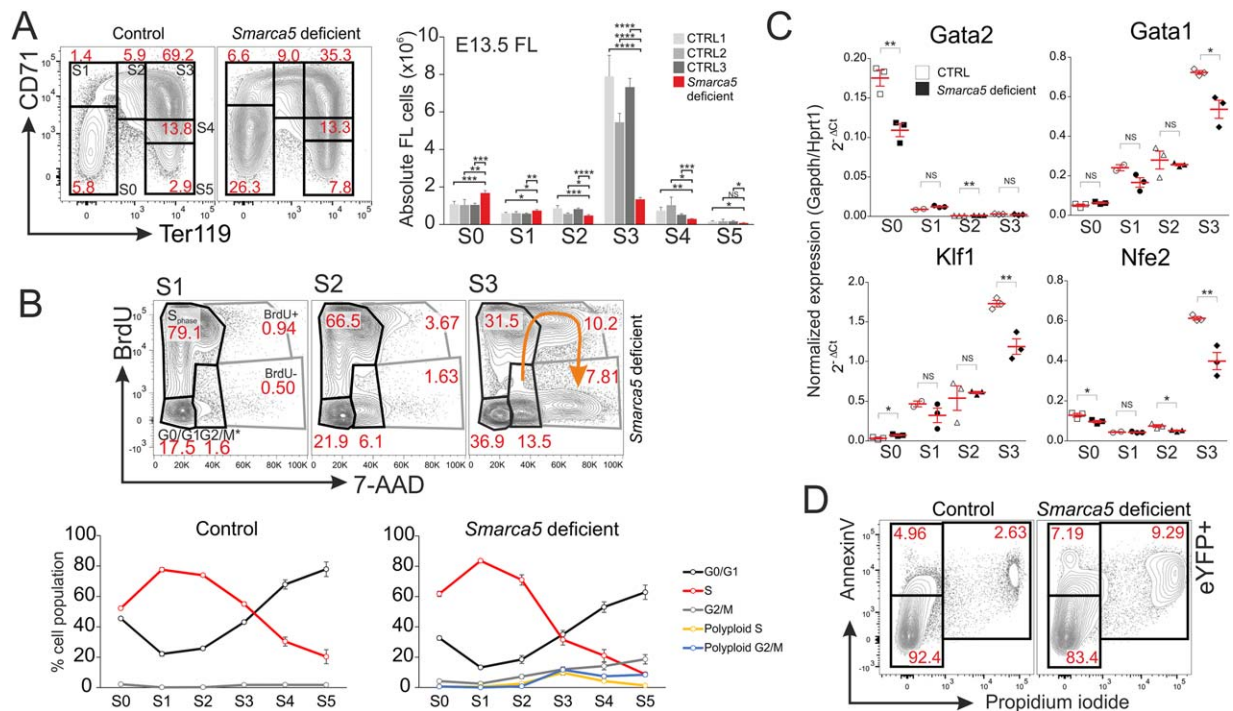


Figure 4. Smarca5 deletion (Vav1-iCre) results in blockade of erythropoiesis. **(A)**: Flow cytometric analysis of Ter119 and CD71 expression in the embryonic day 13.5 (E13.5) fetal livers (FLs). Relative (upper) and absolute (bottom) cell numbers in the E13.5 FL. Mutant: *Smarca5^{fllox5/Δ5-9} Rosa26^{eYFP/+} Vav1-iCre*. Controls: *Smarca5^{fllox5/+} Rosa26^{eYFP/+}*; *Smarca5^{fllox5/Δ5-9} Rosa26^{eYFP/+}*; *Smarca5^{fllox5/+} Rosa26^{eYFP/+} Vav1-iCre*. **(B)**: Evaluation of erythroid cell cycle progression in S1–S3 stages by flow cytometry of BrdU/7-aminoactinomycin D stained E13.5 FL. Bottom: Cell cycle kinetics of progenitor and erythroid cell populations (S0–S5) in control and mutant E13.5 FLs. **(C)**: Quantitative polymerase chain reaction expression of selected hematopoietic/erythroid transcription factors from eYFP+ S0–S3 fluorescence-activated cell sorting-sorted cell populations in E14.5 FL. Controls: *Smarca5^{fllox5/+} Rosa26^{eYFP/+} Vav1-iCre* ($n = 3$) and mutants: *Smarca5^{fllox5/Δ5-9} Rosa26^{eYFP/+} Vav1-iCre* ($n = 3$). **(D)**: Annexin V and propidium iodide staining in the FL eYFP+ fraction of E13.5 FL. Similar results were obtained in at least six repeat experiments. Statistics: two-tailed Student's t test (*, $p < .05$; **, $p < .001$; ***, $p < .0001$; ****, $p < .00001$). Abbreviations: 7-AAD, 7-aminoactinomycin D; BrdU, 5-Bromo-2'-deoxyuridine; CTRL, control; E13.5, embryonic day 13.5; FL, fetal liver.

eYFP+ E14.5 FL-derived S0–S3 stages. We found that all of the assayed p53 target gene mRNAs (*Pmaip/Noxa*, *Gadd45b*, *Cdkn1a/p21*, and *Bbc3/Puma*) are increased in at least one of the erythroid populations from the mutant, whereas *Smarca5* mRNA and *Pten* mRNA are decreased in all mutant populations undergoing erythroid development suggesting that erythroid cells maintained activation of p53 targets upon loss of *Smarca5* (Supporting Information Fig. S4E). Thus, the induction of a DDR pathway associated with *Smarca5* deficiency, observed in mutant HSC/MPP cells, occurs also in *Smarca5* deficient erythroid cells.

Smarca5 Is Needed for Proliferation and Survival of EPs

Our results indicate that *Vav1-iCre*-mediated *Smarca5* deficiency leads to perturbations in cell cycling and inhibition of maturation of HSCs at several stages of development from LSK cells to committed EPs. We next sought to determine whether *Smarca5* is also required at later stages of erythroid development and whether the effects of *Smarca5* deficiency on erythroid development are cell autonomous. To address the effects of *Smarca5* deficiency specifically in erythroid cells, we used the *Epor-iCre* allele that is expressed only in fully committed EPs and their progeny [19]. All genotypes from the mating of *Smarca5^{+/-}Δ5-9 Epor-iCre* and *Smarca5^{fllox5/fllox5}* were born including the *Smarca5^{fllox5/Δ5-9 Epor-iCre}* mice. However, closer examination of pups surviving beyond P9 indicated that the mutants were

underrepresented (Supporting Information Fig. S5A). Newborn *Smarca5^{fllox5/Δ5-9 Epor-iCre}* pups were pale and displayed a variable degree of growth delay and failure to thrive (Fig. 5A). Additional study of embryos showed that indeed the E12.5–E18.5 *Smarca5^{fllox5/Δ5-9 Epor-iCre}* embryos are anemic with reduced overall size and cellularity of the FL (Supporting Information Figs. S5B–S5D). Flow cytometric analysis of FL erythroid cells (S0–S5) showed a similar shift toward the more immature erythroid populations (S0–S1) in *Smarca5^{fllox5/Δ5-9 Epor-iCre}* embryos (Fig. 5B), similar to that seen in *Vav1-iCre* mutant FLs. The S3–S5 populations were decreased in the mutants, although the reductions were not as large as seen in *Smarca5^{fllox5/Δ5-9 Vav1-iCre}* FLs. This was consistent with the cytology examinations, that showed that the *Smarca5^{fllox5/Δ5-9 Epor-iCre}* FLs were (unlike the *Vav1-iCre* mutants) comparably populated (to controls) by proerythroblasts and basophilic erythroblasts (Supporting Information Fig. S5E). Colony formation assays with *Smarca5^{fllox5/Δ5-9 Epor-iCre}* FLs showed reduced BFU-E, CFU-E, and CFU-GEMM (Fig. 5E), although the reductions were again not as large as seen in *Smarca5^{fllox5/Δ5-9 Vav1-iCre}* FLs. Using the *Rosa26-STOP-eYFP* allele, we observed that *Epor-iCre* is active within the S1–S5 FL erythroid populations (Supporting Information Fig. S5H). Consistent with the expression of *Epor* in the definitive erythroid cells, no delay was noted in the embryonic-to-definitive hematopoiesis switch in *Smarca5^{fllox5/Δ5-9 Epor-iCre}* FLs (Supporting Information Fig. S5F).

To investigate the cell proliferation and survival properties of FL erythroid cells that could account for an increase in the

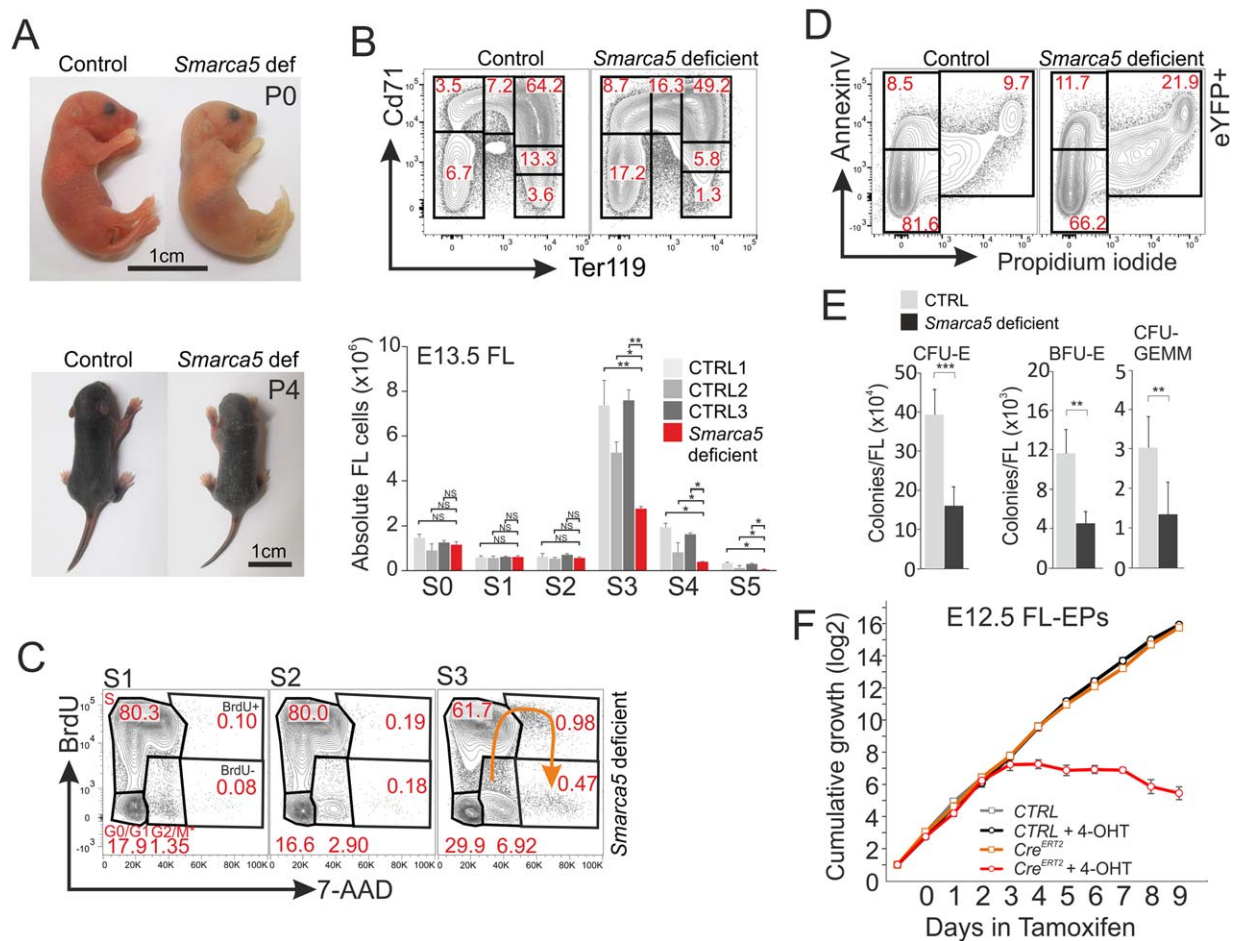


Figure 5. *Smarca5* deletion (*Epor-iCre*) inhibits erythropoiesis. **(A)**: Phenotypic appearance of *Smarca5*^{flx5/+} and *Smarca5*^{flx5/Δ5-9} *Epor*^{+/*eGFP-iCre*} newborns and postnatal day 4 (P4) siblings. **(B)**: Flow cytometric analysis of embryonic day 13.5 (E13.5) fetal liver (FL) cells. Control (*Smarca5*^{flx5/+} *Rosa26*^{eYFP/+} *Epor*^{+/*eGFP-iCre*}) and mutant (*Smarca5*^{flx5/Δ5-9} *Rosa26*^{eYFP/+} *Epor*^{+/*eGFP-iCre*}) FLs. Absolute cell numbers in E13.5 FL in S0–S5 erythroid differentiation stages are shown for controls: (1) *Smarca5*^{flx5/+} *Rosa26*^{eYFP/+}; (2) *Smarca5*^{flx5/Δ5-9} *Rosa26*^{eYFP/+}; (3) *Smarca5*^{flx5/+} *Rosa26*^{eYFP/+} *Epor*^{+/*eGFP-iCre*}, and mutants *Smarca5*^{flx5/Δ5-9} *Rosa26*^{eYFP/+} *Epor*^{+/*eGFP-iCre*}. **(C)**: BrdU labeling of the FL S1–S3 erythroid populations in *Smarca5*^{flx5/Δ5-9} *Rosa26*^{eYFP/+} *Epor*^{+/*eGFP-iCre*} FLs and appearance of polyploid cells. **(D)**: Annexin V and propidium iodide staining in the eYFP⁺ cell fraction of E13.5 FL. Control: *Smarca5*^{flx5/+} *Rosa26*^{eYFP/+} *Epor*^{+/*eGFP-iCre*}; mutant: *Smarca5*^{flx5/Δ5-9} *Rosa26*^{eYFP/+} *Epor*^{+/*eGFP-iCre*}. **(E)**: Colony forming unit numbers from FL-derived progenitors E13.5 of the genotypes same as in Figure 5E. **(F)**: Cumulative growth curve (y-axis log² of 10⁶ cells) of primary FL-derived erythroid progenitors (FL-EPs) prepared from E12.5 control (*Smarca5*^{flx5/flx5}) and 4-hydroxytamoxifen-inducible (4-OHT) (*Smarca5*^{flx5/Δ5-9} *CAG-Cre*^{ERT2}) embryos and grown in serum-free in vitro conditions with or without 4-OHT. control: *Smarca5*^{flx5/flx5}, CRE^{TX}; *Smarca5*^{flx5/Δ5-9} *CAG-Cre*^{ERT2}. Similar results were obtained in at least six repeat experiments. Two-tailed Student's *t* test (*, *p* < .05; **, *p* < .001; ***, *p* < .0001). Abbreviations: 7-AAD, 7-aminoactinomycin D; BFU, Burst-forming unit; BrdU, 5-Bromo-2'-deoxyuridine; CFU, colony forming unit; CTRL, control; E13.5, embryonic day 13.5; EPs, erythroid progenitors; FL, fetal liver.

relative numbers of more immature populations (S0–S1) and a reduction in more mature cells (S3–S5) in *Smarca5*^{flx5/Δ5-9} *Epor-iCre* FLs, we again used in vivo BrdU labeling and flow cytometry combined with 7-AAD, annexin V, and propidium iodide staining. We observed a marked decrease in BrdU incorporation within the S3 compartment and an increase in polyploid cells, although these defects were not as severe as in the *Smarca5*^{flx5/Δ5-9} *Vav1-iCre* FLs (Fig. 5C; Supporting Information Fig. S51). Similarly, to *Vav1-iCre* mutants, there was evidence of increased apoptosis (8.5% vs. 12%) and necrosis (10% vs. 22%) in the *Smarca5*^{flx5/Δ5-9} *Epor-iCre* FLs compared with controls (Fig. 5D).

To determine whether the observed effect of *Smarca5* deficiency in the erythroid compartment is cell autonomous, we used the *Cre-Esr1* allele [9] that promotes Cre-mediated inactivation upon addition of 4-OHT. We isolated FL cells from

E12.5 *Smarca5*^{flx5/Δ5-9} *Cre-Esr1* embryos and cultured them under conditions that promote proliferation of immature EPs for several weeks [8]. Cells were cultured 24 hours before adding 4-OHT. We observed that growth of the cultures was halted quite abruptly 72 hours after addition of 4-OHT (Fig. 5F). These results indicate that *Smarca5* is required in a cell autonomous manner for proliferation of EPs.

DISCUSSION

Smarca5 was previously shown to be an essential factor in early mammalian development [5]. In this work, we have demonstrated that it is required for maturation of definitive HSCs and for completion of erythropoiesis. We observed that mutant *Smarca5* HSC/MPPs accumulate in FLs (Fig. 2B), while the subsequent stages involving LS-K cell proliferation

becomes progressively blocked at early differentiation stage (Fig. 2C) and CFU-forming progenitors are not able to form blood colonies (Fig. 2D). This leads to anemia and fetal stage-lethality before birth. The phenotype is related to the *Smarca5* expression, which is very high in early HSCs and proliferating progenitors and its downregulation occurs during the later stages of erythropoiesis [20].

The erythroid defect in the *Smarca5* mutant mice involved a slowed onset of definitive hematopoiesis and defective proerythroblast-to-basophilic erythroblast maturation (Fig. 4) marked by reduced expression of *Gata1* and its target genes. These observations resemble some properties seen in erythroid cells upon deletion of the erythroid-specific transcription factor *Gata1* [21], suggesting the possibility that *Smarca5* and *Gata1* cooperate during erythroid differentiation. Indeed, *Smarca5* and *Gata1* were previously shown to physically interact in the proerythroblast/basophilic erythroblastic MEL cell line [22]. The fact that the *Smarca5* mutant embryos die later (E18.5) versus previously shown erythroid gene knockouts (E13.5–E15.5) [23] could be caused by later onset of the *Vav1* expression, (which starts at E10.5 [12] and) which is relatively later compared with erythroid genes (e.g., *Epo* and *Epor* expression start around E8.5 and anemic FLs are observed at E11.5). The defect in erythropoiesis in *Smarca5* deficient mice also partly resembles phenotypic outcome of inactivating another chromatin remodeling factor, the SWI/SNF ATPase *Brg1*, that resulted in anemia and embryonic lethality [4], as well as dysregulation of the epigenetic state of the β -globin locus [24, 25]. However, the phenotype of the *Brg1* mutants (compared with the *Smarca5* mutants) involved more differentiated erythroid cells and did not lead to significant accumulation of early progenitors [4]. The erythroid phenotype of *Smarca5* deficiency is consistent with the previously reported SMARCA5 knockdown experiment that caused an inhibition of early erythroid differentiation and led to downregulation of β -globin expression in human CD34+ progenitors and K562 cells [5]. Interestingly, compared with erythropoiesis, the myelopoiesis in the *Smarca5* mutant is affected less severely, consistent with SMARCA5 being a negative regulator of the myeloid transcriptional activator PU.1 [26]. As downregulation of *Gata1* does not directly induce apoptosis [27], we think that the cell death and cell cycle arrest of the *Smarca5*-deficient erythroblasts is rather a result of the loss of *Smarca5* function in cellular pathways other than *Gata1* promoted differentiation. This contention is also supported by the fact that downregulation of erythroid key regulators including *Gata1*, *Gata2*, *Klf1*, and *Nfe2* in the FL kit+ cells and erythroid subpopulations S0–S3 from the YFP-positive fraction of *Smarca5*^{flox5/ Δ 5-9} *Vav1-iCre* mutants (Fig. 4C) was not observed in any of the erythroid fraction of the *Smarca5*^{flox5/ Δ 5-9} *Epor-iCre* mutants (Supporting Information Fig. S5J). This conclusion is also supported by the ex vivo proliferation experiment of *Smarca5*-deficient erythroid cells which showed that *Smarca5* is required for proliferation of EPs (Fig. 5).

Smarca5 deficiency affected cell cycle progression coincidentally with tetraploidy and activation of a DDR. Indeed, as early as the HSC/MPP stage, the loss of *Smarca5* was reflected in the increased proportion of LSK cells entering S-phase (Fig. 2). Furthermore, in the next developmental step, within the LS-K cells, proliferation was markedly reduced coincidentally with G2/M phase accumulation (Fig. 2). Gene

expression analyses at the progenitor level revealed that the most significantly affected transcriptional programs in *Smarca5*-deficient progenitors belonged to stressed hematopoiesis pathways including the p53 target genes (Fig. 3). As expected, the p53 became activated at two residues: S15^{Phos} that was previously associated with DNA damage [17] and the K376 acetylation representing CBP/p300-mediated mark (Fig. 3D). In addition, another DNA damage mark, Kap1 S824^{Phos}, became activated. Interestingly, the levels of Trp53 protein were increased while its inhibitor Mdm2 was reciprocally decreased in the mutants. However, we have not confirmed the *Atm/Atr* pathway activation of Chk1/Chk2 (Supporting Information Fig. S3C) upon *Smarca5* deficiency. We conclude that *Smarca5* deficiency activated two activating modifications of p53. However, our data also show that γ H2AX staining was not enriched in the mutants supporting possibility of more complex mechanism upstream the p53 activation.

Stressed hematopoiesis induced by genotoxic agents in HSC is often coupled with Gadd45a-mediated activation of MPPs followed by erythromegakaryocytic and myelolymphoid differentiation [28]. However, this wave of coordinated proliferation and differentiation does not occur upon *Smarca5* deficiency and instead the mutant cells are blocked from proliferation at the tetraploid state, which prevents further completion of cell differentiation. In addition, a significant proportion of the mutant cells underwent the p53-mediated apoptosis (Fig. 3), which further aggravated the anemic phenotype. Polyploidy was also previously shown to increase tolerance to mitotic errors [29] and may result in appearance of binucleate-like cells [30] that were also readily observable in the mutant FLs. Activation of p53 and its program including induction of p21 as a consequence of polyploidy has been observed experimentally upon addition of microtubule assembly inhibitors [31]. In addition, another activator of p21 was overrepresented in the mutants such as Kap1 S824^{Phos} (Fig. 3D). Interestingly, p21 could be also activated by hypoxia via Hypoxia-inducible factor 1 (HIF-1) [32] supporting the possibility that both p53 and p21 activation could be augmented by severe hypoxia [33] as also documented by activation of the HIF-1 mRNA targets (Supporting Information Fig. S3D). *Smarca5* deficiency thus disrupted the proliferation of HSCs differentiating into erythroid lineage, affecting its development, and causing severe anemia. Tp53 activation appears to be a mediator of the proliferation blockade and apoptosis in the *Smarca5* mutants.

CONCLUSION

Smarca5 deficiency suppressed hematopoietic development and caused erythroid dysplasia and anemia coincident with activation of the p53 and its program. If *Smarca5* is not available, the cell cycle progression becomes progressively inhibited at the MPP level at G2/M phase leading to erythroid defect and severe anemia.

ACKNOWLEDGMENTS

We thank Ivan A. Kanchev, Attila Juhasz, and Marketa Pickova from Czech Centre for Phenogenomics at BIOCEV for their counseling and assistance with histology and the IMCF at BIOCEV, institution supported by the MEYS CR (LM2015062 Czech-BioImaging). This work was primarily supported by GAČR 16-

05649S, AZV 16-27790A, and KONTAKT II LH15170 (to T.S.); NIH GM116143 and DK096266 (to A.I.S.); and GAUK 815316 (to J.K.). Institutional support by UNCE 204021, PRVOUK P24, LQ1604 NPU II, and CZ.1.05/1.1.00/02.0109 (to T.S.).

F.S.: fluorescence-activated cell sorting; W.E.: blastocyst injection and embryonic stem cell transfection; A.I.S. and T.S.: designed the experiments and co-wrote the manuscript, senior co-authors.

AUTHOR CONTRIBUTIONS

J.K.: experimental design, cloning, cell biology, flow cytometry and phenotype analysis; T.Z.: genotyping and mouse colony;

DISCLOSURE OF POTENTIAL CONFLICTS OF INTEREST

The authors indicate no potential conflicts of interest.

REFERENCES

- Erdel F, Rippe K. Chromatin remodelling in mammalian cells by ISWI-type complexes—Where, when and why? *FEBS J* 2011; 278:3608–3618.
- He X, Fan HY, Garlick JD et al. Diverse regulation of SNF2h chromatin remodeling by noncatalytic subunits. *Biochemistry* 2008; 47:7025–7033.
- Lazzaro MA, Picketts DJ. Cloning and characterization of the murine Imitation Switch (ISWI) genes: Differential expression patterns suggest distinct developmental roles for Snf2h and Snf2l. *J Neurochem* 2001;77: 1145–1156.
- Bultman SJ, Gebuhr TC, Magnuson T. A Brg1 mutation that uncouples ATPase activity from chromatin remodeling reveals an essential role for SWI/SNF-related complexes in beta-globin expression and erythroid development. *Genes Dev* 2005;19:2849–2861.
- Stopka T, Skoutlchi AI. The ISWI ATPase Snf2h is required for early mouse development. *Proc Natl Acad Sci USA* 2003;100: 14097–14102.
- Alvarez-Saavedra M, De Repentigny Y, Lagali PS et al. Snf2h-mediated chromatin organization and histone H1 dynamics govern cerebellar morphogenesis and neural maturation. *Nat Commun* 2014;5:4181.
- Shafi R, Iyer SP, Ellies LG et al. The O-GlcNAc transferase gene resides on the X chromosome and is essential for embryonic stem cell viability and mouse ontogeny. *Proc Natl Acad Sci USA* 2000;97:5735–5739.
- Dolznic H, Kolbus A, Leberbauer C et al. Expansion and differentiation of immature mouse and human hematopoietic progenitors. *Meth Mol Med* 2005;105:323–344.
- Hayashi S, McMahan AP. Efficient recombination in diverse tissues by a tamoxifen-inducible form of Cre: A tool for temporally regulated gene activation/inactivation in the mouse. *Dev Biol* 2002;244:305–318.
- Pop R, Shearstone JR, Shen Q et al. A key commitment step in erythropoiesis is synchronized with the cell cycle clock through mutual inhibition between PU.1 and S-phase progression. *PLoS Biol* 2010;8:e1000484.
- Kiel MJ, Yilmaz OH, Iwashita T et al. SLAM family receptors distinguish hematopoietic stem and progenitor cells and reveal endothelial niches for stem cells. *Cell* 2005; 121:1109–1121.
- Munugalavada V, Dore LC, Tan BL et al. Repression of c-kit and its downstream substrates by GATA-1 inhibits cell proliferation during erythroid maturation. *Mol Cell Biol* 2005;25:6747–6759.
- de Boer J, Williams A, Skavdis G et al. Transgenic mice with hematopoietic and lymphoid specific expression of Cre. *Eur J Immunol* 2003;33:314–325.
- Cabezas-Wallscheid N, Klimmeck D, Hansson J et al. Identification of regulatory networks in HSCs and their immediate progeny via integrated proteome, transcriptome, and DNA methylome analysis. *Cell Stem Cell* 2014;15:507–522.
- Oguro H, Ding L, Morrison SJ. SLAM family markers resolve functionally distinct subpopulations of hematopoietic stem cells and multipotent progenitors. *Cell Stem Cell* 2013;13:102–116.
- Srinivas S, Watanabe T, Lin CS et al. Cre reporter strains produced by targeted insertion of EYFP and ECFP into the ROSA26 locus. *BMC Dev Biol* 2001;1:4.
- Ullrich SJ, Sakaguchi K, Lees-Miller SP et al. Phosphorylation at Ser-15 and Ser-392 in mutant p53 molecules from human tumors is altered compared to wild-type p53. *Proc Natl Acad Sci USA* 1993;90:5954–5958.
- Sakaguchi K, Herrera JE, Saito S et al. DNA damage activates p53 through a phosphorylation-acetylation cascade. *Genes Dev* 1998;12:2831–2841.
- Heinrich AC, Pelanda R, Klingmuller U. A mouse model for visualization and conditional mutations in the erythroid lineage. *Blood* 2004;104:659–666.
- Stopka T, Zakova D, Fuchs O et al. Chromatin remodeling gene SMARCA5 is dysregulated in primitive hematopoietic cells of acute leukemia. *Leukemia* 2000;14:1247–1252.
- Fujiwara Y, Browne CP, Cunniff K et al. Arrested development of embryonic red cell precursors in mouse embryos lacking transcription factor GATA-1. *Proc Natl Acad Sci USA* 1996;93:12355–12358.
- Rodriguez P, Bonte E, Krijgsveld J et al. GATA-1 forms distinct activating and repressive complexes in erythroid cells. *EMBO J* 2005;24:2354–2366.
- Wu H, Liu X, Jaenisch R et al. Generation of committed erythroid BFU-E and CFU-E progenitors does not require erythropoietin or the erythropoietin receptor. *Cell* 1995;83: 59–67.
- Armstrong JA, Bieker JJ, Emerson BM. A SWI/SNF-related chromatin remodeling complex, E-RC1, is required for tissue-specific transcriptional regulation by EKLF in vitro. *Cell* 1998;95:93–104.
- O'Neill D, Yang J, Erdjument-Bromage H et al. Tissue-specific and developmental stage-specific DNA binding by a mammalian SWI/SNF complex associated with human fetal-to-adult globin gene switching. *Proc Natl Acad Sci USA* 1999;96:349–354.
- Dluhosova M, Curik N, Vargova J et al. Epigenetic control of SPI1 gene by CTCF and ISWI ATPase SMARCA5. *PLoS One* 2014;9: e87448.
- McDevitt MA, Shivdasani RA, Fujiwara Y et al. A “knockdown” mutation created by cis-element gene targeting reveals the dependence of erythroid cell maturation on the level of transcription factor GATA-1. *Proc Natl Acad Sci USA* 1997;94:6781–6785.
- Wingert S, Thalheimer FB, Haetscher N et al. The DNA-damage response gene GADD45A induces differentiation in hematopoietic stem cells without inhibiting cell cycle or survival. *STEM CELLS* 2016;34:699–710.
- Kuznetsova AY, Seget K, Moeller GK et al. Chromosomal instability, tolerance of mitotic errors and multidrug resistance are promoted by tetraploidization in human cells. *Cell Cycle* 2015;14:2810–2820.
- De Santis Puzzon M, Gonzalez L, Ascenzi S et al. Tetraploid cells produced by absence of substrate adhesion during cytokinesis are limited in their proliferation and enter senescence after DNA replication. *Cell Cycle* 2015;0.
- Andreassen PR, Lohez OD, Lacroix FB et al. Tetraploid state induces p53-dependent arrest of nontransformed mammalian cells in G1. *Mol Biol Cell* 2001;12:1315–1328.
- Carmeliet P, Dor Y, Herbert JM et al. Role of HIF-1alpha in hypoxia-mediated apoptosis, cell proliferation and tumour angiogenesis. *Nature* 1998;394:485–490.
- Zhou CH, Zhang XP, Liu F et al. Modeling the interplay between the HIF-1 and p53 pathways in hypoxia. *Sci Rep* 2015;5:13834.



See www.StemCells.com for supporting information available online.